Proc. Natl. Acad. Sci. USA
Vol. 96, pp. 61–66, January 1999
Biochemistry, Engineering

An arrayable flow-through microcentrifuge for high-throughput instrumentation

ANDRE MARZIALI*, THOMAS D. WILLIS, AND RONALD W. DAVIS

Stanford DNA Sequencing and Technology Center, 855 California Avenue, Palo Alto, CA 94304

Contributed by Ronald W. Davis, November 10, 1998

ABSTRACT **A compact, flow-through centrifugation system has been developed specifically for high-throughput centrifugation of large numbers of samples. The instrument is based on multiple high-speed rotors that also serve as sample holders. The small size of the rotors allows them to be arrayed in a standard 96-well microtiter plate spacing, making this device ideal for highly parallel automated instrumentation. Though initially designed for cell separation in DNA sequencing protocols, the flow-through centrifuge can be used to replace conventional centrifugation in most processes involving small samples. Techniques for recovery of both the supernatant and the pellet have been developed, as well as techniques for sample mixing, and cleaning of the reusable rotors. This paper discusses the design and performance of the flow-through centrifuge applied to cell separation and resuspension and to DNA purification and concentration.**

Centrifugation as a means of accelerating sedimentation of precipitates and particulates has long been an integral part of biochemical protocols. Recently, the increasing demand for high-throughput assays in the field of biochemistry has dictated a need for parallel processing and automation of many such protocols. Standard centrifuges have proven to be incompatible with these needs.

The need for highly parallel sample processing has led the community to usage of multiwell microtiter plates. Because of their insufficient mechanical strength, centrifugation of samples held in such plates is limited to accelerations below $3{,}500 \times g$. Furthermore, microtiter plate centrifuges are large and cumbersome to automate. Though automation of centrifuge-based sample preparation has been performed successfully (ref. 1; AutoGen 740, AutoGen, Framingham, MA), the resulting instruments are inherently low-throughput (<96 samples/hr per instrument) as a result of these difficulties.

Filter-based separation protocols also have been automated by several companies (Qiagen, Chatsworth, CA, and Beckman Coulter) but also are limited in throughput (≈96 samples/hr per instrument) and are more than 10 times more expensive than centrifuge-based separations.

To address this need for high-throughput, automated centrifugation, a centrifuge has been developed in which samples are spun directly in contact with individual, miniature rotors rather than in a sample holder. Thus, the centrifugal field is no longer limited by the strength of the sample tray and can be made to exceed $20{,}000 \times g$. Individual rotors can be arrayed on a standard 96-well spacing (9 mm). This spacing has allowed the development of a 96-channel version of the centrifuge described in this paper, which is capable of processing 96 samples in parallel and dispensing the supernatants or resuspended precipitates directly into a microtiter plate. This device can be loaded by a standard 8-, 12-, or 96- channel pipettor and thus is easily automated. Pelleting times are short because of the high centrifugal field and the short drift distance within the sample. Cleaning of rotors is performed easily and allows their reuse, making protocols executed with this device very inexpensive. This technology therefore meets the need for a compact, inexpensive, and automatable high-throughput centrifugation system.†

Materials and Methods

Rotor Construction. Fig. 1 shows a partial cutaway view of a rotor. The rotors are machined in two halves from titanium rod to tolerances of ± 0.0005 in. The halves are mated together with a press-fit that is augmented with retaining compound. The assembled rotor is 1.2 in. long, with an o.d. of 0.34 in. The internal taper is at a 17° angle to the vertical. The entrance and exit holes are 0.06- to 0.08-in diameter.

The ethanol precipitation experiments were carried out in a flat wall rotor (see Fig. 4*B*). A 1/16-in o.d. Teflon tube is press-fit into the output spout, reducing the diameter of the exit hole to 0.020 in to allow recovery of small volumes.

Support System (Bearings). The rotor shafts mate to flanged ball bearings (0.125-in shaft, 0.250-in o.d., high-temperature ball separator, Micro Miniature Bearing Co., Old Bridge, NJ). These bearings are rated for operation at speeds up to 140,000 rpm. Lubrication is in the form of light synthetic oil. An inner race shaft spacer is used to avoid contact between the rotor and the outer race. The small size of the bearings makes them very sensitive to damage from press-fits. Consequently, the bearings are slip-fit into a stainless steel support plate and bonded with cyanoacrylate adhesive to prevent slippage of the outer race. The top and bottom support plates are separated by an aluminum spacer and aligned with guide pins to within ± 0.001 in.

Drive System. Though the rotors originally were designed to be driven pneumatically, a belt drive system has been developed in collaboration with Genemachines (Menlo Park, CA) to improve rotational uniformity of arrays of rotors. This system uses a lightweight belt (Genemachines) that is wrapped around the rotor and driven by using a brushless servo motor (MicroMo 3564, 100 W). The belt is 0.25 in wide and 0.003 in thick and is wrapped around the equator of the rotor. The drive pulley is crowned to stabilize the belt.

Cleaning Protocols. *Resuspension-based protocols.* The protocol to remove cell debris involved the following. Rotors were filled with 300 μl of wash buffer and made to undergo a resuspension routine (ν_h = 10,000 rpm, ν_l = 1,000 rpm, t = 0.5 s, n = 50). The wash buffer then was expelled from the rotor under pressure. These steps were repeated for a sequence of wash buffers. The first wash buffer was water, and the second

The publication costs of this article were defrayed in part by page charge payment. This article must therefore be hereby marked "*advertisement*" in accordance with 18 U.S.C. §1734 solely to indicate this fact.

*To whom reprint requests should be sent at present address: Department of Physics and Astronomy, Room 415, University of British Columbia, 6224 Agricultural Road, Vancouver, British Columbia, V6T 1Z1, Canada. e-mail: andre@physics.ubc.ca.

†Further information can be obtained from http://sequence-www.stanford.edu.

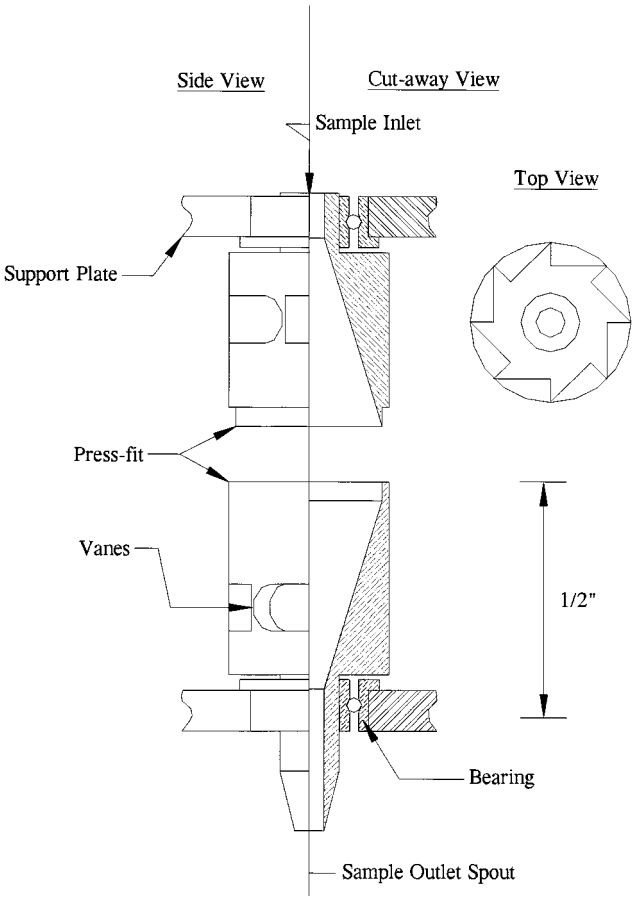

FIG. 1. Cutaway drawing of a rotor showing bearings and inner V profile.

was an alkaline cell lysis buffer (0.2 M NaOH/1% SDS). These two buffers were alternated twice each and then a final water wash was executed followed by a drying step.

The protocol to remove DNA precipitate was the same as above except no alkaline lysis buffer was used. The water wash was iterated five times.

Jet-based cleaning protocol. Rotors are washed by inserting a 21-g hypodermic needle into the rotor and passing high-pressure water through it. The needle bevel is angled so as to direct the jet at the rotor equator. The input water is pressurized to ≈30 psi to achieve a flow rate through the needle of ≈4 ml/s. This flow is maintained for ≈2.5 s while the rotor is slowly rotated (≈600 rpm). The rotor then is dried for 10 s by using compressed air.

Reagents. Cell cultures. All cell cultures used were *Escherichia coli* DH10B strain (GIBCO/BRL). Where specified, they contained pUC 118 plasmids that confer ampicillin resistance. Where specified, these plasmids contain an insert that disrupts the β-galactosidase gene. All cultures were grown in terrific broth (2).

Ethanol precipitation reagents. The reagents used were: 150 μl of Tris-EDTA (10 mM Tris·HCl/1 mM EDTA, pH 8.0) containing 2.5 μg of DNA, 300 μl of 100% ethanol, and 15 μl of 3 M NaAc solution.

The Flow-Through Microcentrifuge

The flow-through centrifuge consists of a miniature cylindrical rotor spinning at high speed around its axis, with entrance and exit holes for the rotor located on-axis at each end (see Figs. 1 and 2). The internal profile of the rotor (typically a V shape) provides a vessel for containing the liquid while the rotor is spinning, and a surface for forming the centrifuged pellet. The rotor is mounted on miniature precision bearings located at its extremities to allow high-speed operation. Two drive systems were developed for the centrifuge: a pneumatic drive and a belt drive. The pneumatic drive consists of an air jet directed at a set of directional vanes cut into the rotor side wall. A second jet, and a second set of vanes in the opposing direction, allows the operator to decelerate the rotor and to drive it in the opposite direction. The jet velocity and rotor speed are regulated by using an electrically controlled proportional valve. This drive system allows the rotor to reach very high speeds because the bearing is not loaded in either the axial or radial directions; however, difficulties with manufacturing uniformity and bearing properties resulted in less than perfect reproducibility of rotor speeds over time and between rotors. To overcome these limitations, a belt drive system was developed in collaboration with Genemachines. In this drive system a high-speed belt is wrapped around the rotor equator and driven by a brushless servo motor. This drive system allows direct control over the rotor speeds and thus was used during most of the tests described in this paper. A photo of the rotors is shown in Fig. 2 and a cross-sectional drawing of an air-driven rotor is shown in Fig. 1.

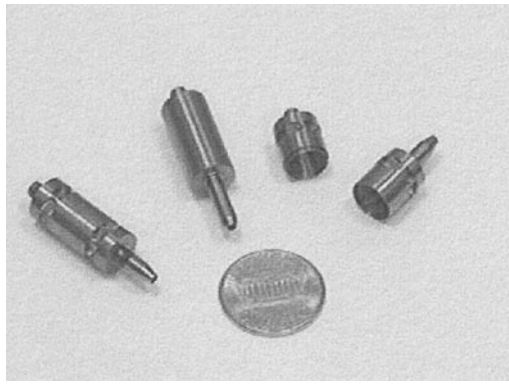

FIG. 2. Titanium rotors: assembled air-driven (*Left*), belt-driven (*Center*), and broken apart (*Right*) to show interior. A penny is shown for scale.

The basic operation of the centrifuge is laid out in Fig. 3. A sample is injected into the spinning rotor via an angled injection needle. The centrifugal force immediately pushes the sample against the rotor wall, preventing it from dripping out the bottom of the rotor. The interior wall taper forces the pellet to accumulate in a ring around the rotor equator. When the pelleting is complete, the rotor is stopped and the supernatant flows out through the bottom spout.

There are several advantages to this geometry. First, the high centrifugal force and short drift distance allows very fast centrifugation times. Second, the small rotor diameter allows highly parallel arrays of centrifuge rotors to be operated, yielding a device that conforms to the industry standard sample spacing for 96-well microtiter plates. Finally, the rotors can be washed and reused. All of these attributes make this technology ideal for automating centrifugation as part of high-throughput instrumentation.

Theory of Operation

Pelleting. The centripetal acceleration in a rotating object is given by $a = \omega^2 r$, where r is the radius of the orbit and ω is the angular velocity. Consequently, pelleting accelerations decrease linearly with decreasing radius but increase quadratically with increasing angular velocity. Because the speed rating of a bearing is inversely proportional to its size,

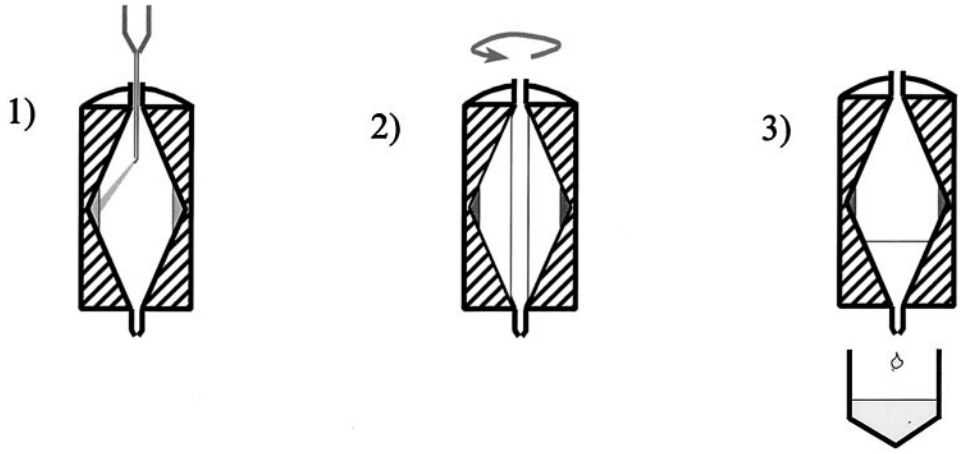

FIG. 3. Cutaway view of a rotor showing the basic mode of operation. The sample is injected into the spinning rotor (*Left*) and is pushed onto the inner surface of the rotor by centrifugal force. The rotor is spun until a pellet forms at the equator (*Center*), and then is decelerated to allow the supernatant to drip out the bottom spout (*Right*).

$$\omega_{\max} \propto \frac{1}{R_{\text{mean}}},$$

it follows that decreasing the size of a centrifuge rotor leads to the possibility for higher angular velocities and greater centrifugal fields.

In the flow-through centrifuge geometry, the small size and mass of the rotor allows the use of a miniature bearing. In a conventional centrifuge, bearing forces caused by unbalanced loading easily can result in hundreds of kilograms of force. However, in the flow-through centrifuge, such unbalanced loads are limited to any rotor nonuniformities, which, given a rotor mass of ≈3 g, can total only ≈0.03 g and lead to radial bearing loads of less than 1 kg. The prototype described herein uses a bearing with 0.125-in bore and an o.d. of 0.25 in. Dental bearings in this size are capable of obtaining rotational speeds in excess of 300,000 rpm; the less-expensive bearings used in this device safely reach speeds of 70,000 rpm and are rated to 15 kg of radial dynamic load.

The result of these considerations is that a centrifuge of the type described above can obtain pelleting accelerations of more than 20,000 × *g* at the equatorial rim at 70,000 rpm. This acceleration compares quite favorably with the ≈3,000 × *g* available in a conventional centrifuge. It should be noted, however, that this pelleting acceleration is available only at the equatorial rim. Given a rotor inlet i.d. of 0.08 in, the pelleting acceleration at the surface of the liquid meniscus when the centrifuge is full is only 5,570 × *g*.

A more useful measure of centrifugation efficiency is, therefore, the time it takes to pellet a given suspension. The drift velocity of a suspended particle in a centrifuge is determined by the balance between the centrifugal force and the sum of the buoyant force and the drag forces. This balance determines the sedimentation coefficient (*S*, in Svedbergs 10^{-13} s), which is simply the proportionality constant between the pelleting acceleration and drift velocity (*V*): $V = Sa$. The time required to pellet a given suspension in a flow-through centrifuge is thus given by,

$$t = \int_{R_{\min}}^{R_{\max}} \frac{dr}{Sa(r)} = \int_{R_{\min}}^{R_{\max}} \frac{R_{\max}}{Sa_{\max}} \frac{dr}{r} = \frac{R_{\max}}{Sa_{\max}} \ln\left(\frac{R_{\max}}{R_{\min}}\right),$$

where, $R_{\max}$ is the outer radius and $a_{\max}$ is the pelleting acceleration at this position. $R_{\min}$ is the radius of the liquid surface. In the case of a conventional plate centrifuge, the pelleting acceleration is essentially constant over the volume, giving a pelleting time of:

$$t = \frac{h}{Sa_{\max}},$$

where $h = R_{\max} - R_{\min}$ is the height of the sample being pelleted.

By using these equations, the time required to pellet a 300-μl culture of *E. coli* cells (which have a sedimentation coefficient of approximately 10^5 Sv) can be calculated and compared. Using the flow-through microcentrifuge (flat wall design, see Fig. 4*B*) rotating at 70,000 rpm, and for the given volume: $R_{\max} = 0.145$ in, $R_{\min} = 0.103$ in, and $t = 0.6$ s (flow-through centrifuge), whereas using a conventional 96-well plate centrifuge with 3,000 g of pelleting force, $h = 7.8$ mm and $t = 26.5$ s (microtiter plate centrifuge). The net result is that the flow-through geometry provides a 40-fold improvement in pelleting times over standard microtiter plate centrifuges. Beyond this basic improvement in drift time is the advantage that, if desired, pellets in the flow-through centrifuge can be compressed under an acceleration that is six times greater than in a conventional centrifuge, leading to a decreased likelihood of pellet resuspension and loss during supernatant removal.

Pellet Retention. To make use of this pelleting efficiency, it is necessary to avoid pellet resuspension as the centrifuge is decelerated. In this geometry, torque is transmitted through shear force from the wall on which the pellet resides. As a result, the pellet experiences a force tangential to the wall surface that must be counteracted by adhesion forces within

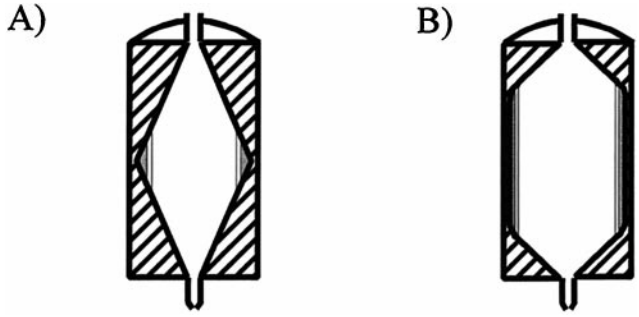

FIG. 4. Resuspension in small volumes requires a compact pellet if the rotor has a tapered interior (*A*) as the resuspension buffer will wet the area only near the equator. If a pellet has not fully compacted into the equator of the rotor, it will not be fully covered by resuspension buffer. In a rotor with flat side walls (*B*), the resuspension buffer will be spread over the entire interior surface, covering the entire surface area of the pellet.

the pellet to avoid resuspension. The adhesion forces are likely to be proportional to the pelleting force (i.e., if the pellet is being compacted it is less likely to resuspend) and the shear forces are proportional to velocity gradients in the flow profile near the wall. In regimes of laminar flow, these can be calculated, but when the flow becomes turbulent, additional and larger forces are present.

These constraints can be summed up by two equations. The shearing condition can be expressed,

$$\frac{\partial V(R,\,t)}{\partial r} < \frac{M_{\text{pellet}}}{\mu A_{\text{pellet}}}\left(k_{\text{normal}}\frac{V_{\text{rotor}}^2}{R} + K_{\text{self-adhesion}}\right),$$

where V is the tangential velocity of the liquid, M_{pellet} is the mass of the pellet, A_{pellet} is the area of the pellet, μ is the viscosity of the solution, k_{normal} is a measure of the pellet adhesion in the presence of a normal force, and $K_{\text{self-adhesion}}$ is a measure of the ability of the pellet to remain intact without the presence of pelleting forces.

The turbulence condition is given by a constraint on the Reynolds number ($\mathcal{R}$),

$$\mathcal{R} = \frac{\rho}{\mu}h(\bar{V} - V_{\text{rotor}}),$$

where ρ is the solution density and h is the depth of the sample and $\bar{V}$ is the average azimuthal liquid velocity. If $\mathcal{R}$ exceeds 4,000 the liquid is likely to flow turbulently across the pellet and will resuspend it.

Simple numerical calculations can be performed to characterize the flow under varying ramp-down profiles. For sufficiently gradual linear decelerations,

$$\frac{\partial V}{\partial r} \propto \frac{dv}{dt}; \qquad \frac{dv}{dt} < \frac{M_{\text{pellet}}}{\mu A_{\text{pellet}}}(k'v^2 + K'),$$

and, $\mathcal{R}$ is constant. In this model, k' and K' need to be determined experimentally to optimize the deceleration profile. Nonturbulent flow occurs only for spin-down rates of,

$$\frac{dv}{dt} \leq 500 \text{ rpm/s}.$$

A gradual linear spin-down therefore will remain nonturbulent. Experimental results confirm that it is particularly important to be in this regime at low rpm where pelleting forces vanish.

Pellet Resuspension and Recovery. Although the shear forces described above necessitate careful control over deceleration profiles, they also give the instrument the ability to resuspend harvested pellets. Any velocity profile that includes sudden accelerations and decelerations of the rotor can be used to maximize the turbulent shear across the pellet in much the same manner as a vortexer. Typical velocity profiles for resuspension consist of rapid velocity cycling between 30,000 rpm and near 0 rpm. The dwell time at low rpm is short enough to ensure that no liquid flows through the exit spout during that part of the cycle. The deceleration from 30,000 rpm to 0 rpm can be accomplished in 0.5 s, yielding a Reynolds number of 480,000 and insuring highly turbulent flow over the pellet.

Redissolving DNA Pellets. Soluble material also can be resuspended by dissolving the pellet in an elution buffer. An example of this process is the concentration of DNA using ethanol precipitation. Because a high concentration of DNA is usually desired, the precipitated DNA pellet should be dissolved in the smallest possible volume.

This process places several constraints on the rotor design. In a V-shaped rotor such as that shown in Fig. 4*A*, a small volume of resuspension buffer will come into contact only with a narrow ring of the internal rotor surface as shown. As long as the pellet is entirely contained within this ring, efficient elution is possible. As already has been calculated, centrifugal force will quickly push the sediment to the side wall. Once the pelleted material reaches the side wall, however, the force pushing the pellet toward the equator is decreased by the shallow angle of the wall and is partially counteracted by adhesion resulting from the normal force acting to press the material into the wall. As a result, depending on the relative adhesion characteristics of the material being pelleted, the time to form such a compact pellet can be far longer than the pelleting time calculated above.

Furthermore, small volumes of elution buffer can form stable droplets in a cleft such as exists at the equator in a V-shape rotor. If this happens, the minimum recoverable volume is determined by the volume required to make such droplets unstable so they can flow out the exit spout.

A possible solution to these problems is suggested in Fig. 4*B*, which shows an alternative internal rotor geometry in which the side wall is flat over much of its longitudinal length. In this geometry, a thin layer of elution buffer can be made to contact the entire rotor surface. This geometry eliminates the need to wait until the pellet forms a compact ring before elution, allowing shorter pelleting times. At the same time, this geometry eliminates the sharp clefts that tend to decrease the stability of small droplets.

It should be noted, however, that this adjustment is not without tradeoffs. As a result of spreading the pellet so thinly, its area is increased, making it more likely to resuspend at slow speeds.

Rotor Cleaning. Reuse of the flow-through centrifuge rotors requires adequate cleaning of the rotor interior. Though it may be possible to manufacture disposable multirotor cartridges or removable rotor inserts, most protocols would benefit from the decreased cost of a reusable system. As a result, a washing protocol is required to allow successive samples to be processed in the same rotor without significant cross contamination. Two essential types of wash have been used: mechanical and chemical.

Mechanical washing consists of mating a nozzle to the entrance hole of the stationary rotor and injecting a high-velocity water jet into the rotor. This wash is sufficient for removing any cell debris and possible contaminants from the interior of the rotor and allows multiple samples to be processed without cross contamination. Nevertheless, the pellet-to-rotor-surface adhesion properties of a brand-new rotor cannot be restored with this wash alone. This effect is presumed to result from a thin protein coat on the rotor inner surface that cannot be removed with a water wash.

For this purpose, chemically reactive washes have been tested, including 10% HCl, which have been found to successfully restore the original surface properties of the rotor. As cross contamination can be suppressed with a simple water wash, the necessity for chemical washes will be determined by the protocol to be executed and its dependence on the rotor surface properties.

Results

Pelleting. Cell pelleting tests were conducted by using cultures of *E. coli* cells grown in terrific broth (2). The rotor was spun up to its pelleting speed (ν), and a 300-μl cell culture was loaded, spun for a time (t_p), then spun down at a constant rate ($d\nu/dt$). The supernatant was collected. Optical density measurements at 600 nm then were made of the starting culture and the supernatant relative to the sterile cell medium. All starting cell cultures had an OD_{600} of 10.0.

During use of a V-shape rotor, 99.5% pellet retention was obtained (ν = 60,000 rpm, t_p = 15 s, $d\nu/dt$ = 500 rpm/s). Furthermore, the final 70 μl of supernatant cleared from the rotor contained the bulk of the resuspended material. If this

liquid is sacrificed, the purity of the supernatant increases to one part in 1,000 (99.9%). Many factors were observed to affect the supernatant purity. Increasing the spin-down rate was clearly seen to degrade the supernatant purity. Following the same protocol reported above and substituting a spin-down rate of $d\nu/dt$ = 2,000 rpm/s yielded a supernatant purity of 90–95%. This purity could be improved (99%) by slowing the ramp at 15,000 rpm to rates of 500 rpm/s or lower. This finding suggests that the pellet can withstand turbulent flows at high speeds when the pelleting force is high but not at low speeds when the pelleting force vanishes.

Self-adhesion properties of the pelleted material were among the other factors that were observed to affect supernatant purity. Older cell cultures that had begun to lyse were more easily pelleted, presumably because the lysed material resulted in a more cohesive pellet. Surface interactions between the pellet and the rotor wall also led to a measurable effect on supernatant purity. New rotors or those subjected to a violent cleaning protocol (10% HCl for 1 min) were observed to yield consistently cleaner supernatants. It is concluded that cellular residue on the rotor surface decreases the adhesion of the pellet to the rotor wall, thus increasing the rate of resuspension.

Experiments also were carried out in a flat-wall rotor. As expected, this rotor geometry does not retain pellets as efficiently as the V-shaped rotor. Optimal conditions were found to yield purities of 99.0% (ν = 60,000 rpm, t_p = 15 s, $d\nu/dt$ = 330 rpm/s). Furthermore, these rotors were observed to be affected to a greater extent by the various adhesion constants discussed above and are recommended only in applications in which supernatant purity is not critical, or in which pellet self-adhesion ensures such purity.

Resuspension. Cell resuspension tests were carried out by using the pelleted cell cultures described above. Resuspension was carried out in a volume (V) of terrific broth cell medium and involved cycling between a high spin velocity (ν_h) and a low spin velocity (ν_l) with a cycle time of (t) s. This procedure was repeated for a given number of cycles (n). Again cell yields were determined by spectrophotometry.

If 300 μl of resuspension buffer was used (V = 300 μl), resuspensions of 100% efficiency were not difficult to obtain. Typical values for our resuspension protocols were: ν_h = 10,000 rpm, ν_l = 1,000 rpm, t = 0.5 s, $n > 10$. It was necessary to keep $\nu_l > 0$ so as not to cross the zero point, which would result in a loss of supernatant. If the resuspension volume is decreased 100 μl, more cycles were needed to obtain 100% pellet recovery ($n > 50$).

Resuspension also was tested in a flat wall rotor. Here again resuspension in 300 μl was easily accomplished with 100% efficiency. Resuspension in 100 μl was more difficult. In this case the resuspension buffer is spread in a very thin layer (0.020 in) across the pellet in which it is hard to generate turbulence. This problem is compounded by the fact that the viscosity of the liquid increases as the pellet resuspends. Two adjustments were made to obtain 100% efficiency in this geometry. The protocol was adjusted (ν_h = 5,000 rpm, ν_l = −5,000 rpm, t = 0.5 s, $n > 50$) to cross the zero point so as to minimize any pelleting force that would tend to offset the resuspension force. This adjustment was made possible by the fact that the small volume and high viscosity of the resuspension solution did not tend to drip out as the rotor crossed the zero point. In addition, the pelleting step itself had to be adjusted so as not to overly pack the pellet (ν = 20,000 rpm, t_p = 5 s, $d\nu/dt$ = 500 rpm/s). It should be noted, however, that this pelleting protocol resulted in the loss of an average of 2% of each pellet.

DNA Precipitation and Concentration. A typical ethanol precipitation protocol was tested by using purified M13 DNA (Amersham Pharmacia). Purified DNA (2.5 μg) was diluted to 150 μl with 1× Tris-EDTA and mixed with 300 μl of ethanol and 4.5 μl of 3 M $NaCH_3CO_2$ solution. The mixture was loaded into a rotor spinning at ν, the solution was spun for a time (t_p), and then spun down to zero velocity at a rate of ($d\nu/dt$). After the supernatant was allowed to drain, 450 μl of 70% ethanol then was loaded into the spinning centrifuge and the same pelleting protocol was repeated. The pellet was dried by passing air through the rotor for 1 min. Finally, 60 μl of 1× Tris-EDTA was dispensed into the rotor, which was spun at 20,000 rpm for 1 min to allow the DNA to redissolve. The sample was collected through a Teflon spout (0.020-in i.d.). To collect the sample in a small volume, a flat wall rotor was used to perform this test. Spectrophotometry at 260 nm was performed on the samples collected. These values were compared with the control sample that contained 2.5 μg of DNA in 60 μl of Tris-EDTA.

Spectrophotometric measurements indicated that it is possible to obtain 100% efficiency in DNA pelleting and resuspension for: ν = 60,000 rpm, t_p = 180 s, $d\nu/dt$ = 330 rpm/s. This efficiency was determined by comparison of the concentration of the redissolved DNA to that of the control sample. Reducing the pelleting time to 30 s decreases the efficiency of recovery to 90%, and increasing the spin-down rate to 2,000 rpm/s decreases the recovery to 80%. This device therefore is capable of performing fast, easily automated ethanol precipitations.

It is important to note that although the pelleting efficiency is high, the volume recovery from the rotor is not perfect. Typically, 45–50 μl of the elution buffer is recovered from the rotor, which implies that 15–25% of the sample is left behind in the rotor. Because this effect is a result of the elution buffer wetting the rotor walls, a Teflon-coated rotor may allow a more efficient recovery of small volumes although such a modification would require the pelleting routines to be re-evaluated because the surface adhesion constants would be modified.

Cleaning and Cross Contamination. The titanium rotor surface is compatible with a wide variety of wash protocols. Several wash buffers have been evaluated as well as two types of wash procedures. In the first, the rotor is filled with a series of wash buffers while undergoing a resuspension protocol of the type described above. The second procedure involved subjecting the interior rotor surface to a high-pressure jet of wash fluid introduced via an angled hypodermic needle.

Results of the cleaning protocols were assayed in several ways. After a cell pelleting step, the rotor was cleaned and 300 μl of sterile terrific broth was introduced into the rotor that was made to undergo a resuspension routine. The supernatant then was collected, and its OD_{600} was measured. To assay cleaning efficiency after a DNA pelleting step, the rotor was washed and 60 μl of water was introduced into the rotor, which was again put through a resuspension routine. This 60-μl sample then was loaded onto an agarose gel to determine whether any DNA was present. In all cases, for the washing protocols listed in *Materials and Methods*, the level of cellular and DNA cross contamination was too small to be measured.

A more sensitive test was performed to measure cross contamination during successive ethanol precipitations. Purified pUC18 was pelleted and eluted. The rotor was washed and a second pUC18 clone containing a 10-kB insert was pelleted and resuspended. DNA from this second purification was electroporated into *E. coli* cells (DH10BS strain, GIBCO/BRL) and the resulting cells were titered on ampicillin agar plates containing 5-bromo-4-chloro-3-indolyl β-D-galactoside to assay for β-galactosidase expression. Cross contamination then could be determined from the ratio of blue colonies to white colonies on the agar plates. The resulting contamination was measured to be 1:1,000.

Discussion

A powerful device has been demonstrated that is capable of automatically carrying out centrifugation-based protocols. The

device presented operates more efficiently than conventional centrifuges and is more easily automated than such instruments.

As previously discussed, the flow-through centrifuge rotor is designed to be arrayed on a standard 96-well spacing (9 mm). A prototype of a 96-well array centrifuge has been constructed and currently is being tested. Issues that should be explored include: bearing selection, lubrication, and lifetime requirements; 96 rotor drive optimization and lifetime; optimal rotor design; centrifugation protocol development; manufacturing requirements; and cost.

We gratefully acknowledge the members of the Stanford DNA Sequencing and Technology Development Center for relevant discussions and suggestions, Genemachines for its significant contributions to this technology, and Bill Sabala for help with manufacturing issues. This research is supported by National Human Genome Research Institute Grant P01-HG-00205.

1. Garner, H. R., Armstrong, B. & Kramarsky, D. A. (1992) *Genet. Anal. Technol. Appl.* **9**, 134–139.
2. Sambrook, I., Fritsch, E. F. & Maniatis, T. (1989) *Molecular Cloning: A Laboratory Manual (*Cold Spring Harbor Lab. Press, Plainview, NY), 2nd Ed.